Intramolecular Dihydrogen Bonding in Main Group Elements. Connection with Dehydrogenation Reactions

Sudhir A. Kulkarni[†]

R & D Center, Mahindra British Telecom Limited, 155 Mumbai-Pune Road, P.O. Box 1119, Pimpri, Pune 411 018, India, and Department of Chemistry, University of Pune, Pune 411 007, India

Received: June 29, 1999; In Final Form: September 16, 1999

The existence of intramolecular dihydrogen bonding in the main group elements is investigated at the ab initio level of theory. The AH_n-XH_m complexes (with A = Li/B/Al and X= F/O/N/Cl/S/P) in general do not show intramolecular dihydrogen bond (DHB) in their equilibrium structures; however, it is observed in the transition state for the dehydrogenation reaction $AH_n-XH_m \rightarrow AH_{n-1}-XH_{m-1} + H_2$. The barriers to these reactions have been calculated and are found to be least for the complexes having DHB in the equilibrium structure or having eclipsed geometry favorable for DHB formation. The topological analysis of electron density distribution provides crucial information on the existence of DHB as well as on the extent of the dehydrogenation reaction. The above features indicate that the motivation for the formation of intramolecular DHB is likely to facilitate the dehydrogenation reaction from complexes similar to AH_n-XH_m.

1. Introduction

Hydrogen bonding is known to be one of the most important weak interactions having significant effect on the structures of compounds in solid, liquid, and gas phases. In general, inter- as well as intramolecular hydrogen bonding provides additional stabilization to the structure, leading to a profound impact on the physical and chemical properties of compounds.[1] An analogous novel type of weak interaction has been identified recently[2] as dihydrogen bond (DHB), a bond of type M−H···H−X, where M is a transition metal and X is an electronegative atom or a group. Transition metal complexes exhibit both intra- as well as intermolecular DHB.[2] This type of intermolecular DH bonding has also been found in the complexes of main group elements and their dimers.[3] Recently, we have systematically studied the occurrence of DHB in the complexes and dimers of second- and third-row hydrides.[4] There exist several transition metal complexes that are stabilized by intramolecular DH bonding.[5] However, compounds exhibiting intramolecular DH bonding in the main group elements are rather uncommon. Crabtree[2] has attributed this to the transient intermediate nature of DH-bonded systems, which readily lose H_2. Atwood et al.[6] have recently reported a structure of 2,2,6,6-tetramethylpiperidine−alane complex (cf. Chart 1) that is stabilized by intramolecular H···H bond. The H···H distance in this complex was reported to be 2.31 Å. This complex readily undergoes dehydrogenation and has been viewed as a transition state prior to dehydrogenation. Similar intramolecular DHB has been proposed in azolylborane adducts with C−H···H−B bonding from their X-ray and NMR studies.[7]

In view of the above facts, it is imperative to investigate the occurrence of intramolecular DHB and its role in the dehydrogenation reaction. It is expected that transition-state structures for the dehydrogenation reactions might involve intramolecular DHB.[6] We have investigated the dehydrogenation reaction paths of several model complexes of second- and third-row hydrides of the type AH_n-XH_m with A being Li/B/Al and X being F/Cl/O/S/N/P. These simple systems could serve as a reasonable model for the compounds that undergo dehydrogenation via stable intramolecular DHB.

CHART 1

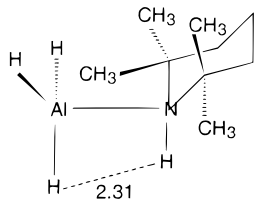

The methodology used herein is discussed in the next section, and the structural features and energetics of dehydrogenation reactions are discussed in section 3. In section 4, we discuss the bonding features of transition-state structures of the dehydrogenation reaction using topological analysis of electron density, and concluding remarks have been made in section 5.

2. Methodology

The equilibrium structures for AH_n-XH_m complexes (with A being Li/B/Al and X being F/Cl/O/S/N/P) have been obtained at the MP2/6-31++g(d,p) and MP2/6-311++G(2d,2p) levels using Gaussian 94.[8] An attempt has been made to obtain stationary structures of these complexes with eclipsed geometry wherein the dihedral angle H−A···X−H is close to 0°. Further, transition-state structures for the dehydrogenation reaction starting from these complexes have been obtained. The nature of stationary points has been confirmed from vibrational frequency calculations at the respective levels of MP2 theory. That these transition states (TS) indeed correspond to dehydrogenation from the complexes have been verified from intrinsic reaction coordinate (IRC) calculations at the MP2/6-31++G(d,p) level. The energy barriers to dehydrogenation reactions have also been obtained from single-point calculations of transition states and complexes, which incorporate higher contributions to the correlation energy. This includes Moller−

[†] E-mail: sudhirk@mahindrabt.com.

10.1021/jp992206w CCC: $18.00
Published on Web 11/03/1999

TABLE 1: Energy Barriers, E_a (kcal/mol), for Dehydrogenation Reaction of Complexes AH_n-XH_m Involving Intramolecular Dihydrogen Bonding as a Transition State at the MP2/6-31++G(d,p) and MP2/6-311++G(2d,2p) Level (in Italics) Geometries

complex	E_a (MP2)	E_a (MP2+ZPE)	E_a (MP3+ZPE)	E_a (MP4SDQ+ZPE)	E_a (CCSD+ZPE)	E_a (CCSDT+ZPE)
$LiH-H_2O$	00.48	−1.34	00.27	00.42	00.11	−0.36
	00.78	*−1.28*	*00.80*	*00.37*	*00.69*	*00.03*
$LiH-H_2S$	2.12	1.92	2.71	3.10	3.36	2.76
	0.55	*0.59*	*0.84*	*1.05*	*1.14*	*0.84*
BH_3-HF	14.71	14.95	18.49	17.03	17.97	16.31
	15.87	*15.63*	*19.35*	*19.39*	*19.24*	*17.25*
BH_3-H_2O	24.96	22.51	25.50	24.78	25.29	24.06
	24.66	*22.15*	*25.53*	*24.82*	*25.22*	*23.68*
BH_3-NH_3	40.81	36.91	39.12	39.01	39.20	38.25
	40.59	*36.54*	*38.95*	*38.92*	*39.81*	*38.82*
BH_3-HCl	12.50	13.00	15.50	15.98	16.29	14.43
	11.06	*10.87*	*13.38*	*13.99*	*14.23*	*12.32*
BH_3-H_2S	19.23	17.73	19.26	19.83	21.29	19.11
	19.05	*17.30*	*19.13*	*19.89*	*20.09*	*18.68*
AlH_3-HF	02.72	01.98	03.83	03.02	03.51	02.70
	03.26	*02.19*	*04.63*	*03.96*	*04.34*	*03.32*
AlH_3-H_2O	17.44	15.40	18.45	17.59	18.03	16.96
	16.40	*14.33*	*17.80*	*17.11*	*17.54*	*16.19*
AlH_3-NH_3	34.21	30.81	33.40	33.11	33.35	32.26
	32.16	*28.76*	*31.68*	*31.62*	*31.90*	*30.49*
AlH_3-HCl	06.83	06.54	07.69	08.04	08.24	07.24
	04.70	*04.17*	*05.66*	*06.20*	*06.37*	*05.29*
AlH_3-H_2S	17.23	17.86	19.12	19.68	20.12	18.87
	14.85	*12.49*	*14.26*	*15.32*	*15.51*	*14.02*
AlH_3-PH_3	42.54	40.07	40.87	41.53	41.88	40.55
	40.24	*37.88*	*39.02*	*40.03*	*40.67*	*38.97*

Plesset perturbative calculations up to third order and fourth order without inclusion of triples (MP3, MP4SDQ) as well as coupled-cluster calculations including singles and doubles (CCSD) as well as singles, doubles, and triples in a noniterative way (CCSDT).

The bonding features of the dihydrogen-bonded TS have been studied with the aid of topographical analysis of their electron density (ED) distribution.[9] Such studies are vital for the knowledge of extent of reaction as well as nature of dihydrogen bonding in the TS. For some of the TS, the atoms in molecule (AIM) approach in Gaussian 94 could not result in identification of DHB, leading to the nonvalidity of the Poincare−Hopf relationship.[10] Therefore, ED analysis using the program UNIPROP[10] was used to verify and correct ED topography in such situations. To understand the driving force behind this reaction, the atomic charges of TS from Mulliken and those from natural population analysis[11] have been used.

3. Results and Discussion

In the present work, an attempt has been made to assess the intramolecular DHB and its connection with the dehydrogenation reactions, viz. $AH_n-XH_m \rightarrow AH_{n-1}-XH_{m-1} + H_2$. The optimized structures of AH_n-XH_m complexes (A = Li/B/Al and X = F/Cl/O/S/N/P) reveal that the majority of complexes are minima with staggered geometry, with the H−A···X−H dihedral angle close to 180°. The equilibrium geometries of some of these complexes at the MP2/6-31++G(d,p) level have been portrayed and discussed in our earlier work.[4] In most of the cases, the structural parameters of these complexes at the MP2/6-311++G(2d,2p) level are quite similar to the earlier reported ones. The energy barriers for the dehydrogenation reaction of AH_n-XH_m complexes at the MP2/6-311++G(2d,-2p) level are reported in Table 1, whereas the corresponding energies of reaction are reported in Table 2.

3.A. Dehydrogenation from $LiH-XH_m$ complexes. The equilibrium and transition-state structures of $LiH-XH_m$ complexes are shown in Figure 1. For $LiH-H_2O$, two structures were reported in our earlier studies,[4] with one involving intramolecular DHB with H···H bond of 1.674 and 1.580 Å at the 6-31++G(d,p) and 6-311++G(2d,2p) levels, respectively. The corresponding H···H distances in the transition states are 1.212 and 1.165 Å, respectively (cf. Figure 1). The O−Li−H angle is reduced by 7.1°, whereas the (Li)H···H−O angle widens by 12.5° in the TS compared to that in the $LiH-H_2O$ complex. Since the $LiH-H_2O$ has DHB in the equilibrium structure and is reasonably stabilized, it is expected to readily undergo the dehydrogenation reaction. This can be verified from meager energy barriers to dehydrogenation of $LiH-H_2O$ from Table 1. On the other hand, the $LiH-H_2S$ complex does not contain the DHB in its equilibrium structure and its TS has a long H···H distance (cf. Figure 1). Because of these structural features, the $LiH-H_2S$ requires more energy for dehydrogenation compared to $LiH-H_2O$, as can be seen from Table 1. Further, the TSs for dehydrogenation from other complexes $LiH-NH_3$ and $LiH-PH_3$ were not found and the stable complexes of LiH with HF and HCl do not exist.[4]

TABLE 2: Energies (kcal/mol) of Dehydrogenation Reactions Including ZPE of AH_n-XH_m Complexes at the MP2/6-311++G(2d,2p) Level Geometry

complex	MP2	MP3	MP4SDQ	CCSD	CCSDT
$LiH-H_2O$	−17.97	−13.91	−15.39	−14.98	−15.10
$LiH-H_2S$	−30.18	−27.69	−26.65	−26.97	−27.47
BH_3-HF	−30.34	−28.57	−29.58	−29.38	−29.35
BH_3-H_2O	−22.85	−21.66	−22.34	−22.60	−22.28
BH_3-NH_3	−8.14	−6.91	−7.57	−7.07	−6.75
BH_3-HCl	−20.04	−18.12	−18.34	−18.62	−18.58
BH_3-H_2S	−11.20	−10.27	−10.64	−11.06	−10.71
AlH_3-HF	−35.50	−32.60	−33.73	−33.27	−33.32
AlH_3-H_2O	−15.53	−12.09	−13.23	−13.28	−13.47
AlH_3-NH_3	2.06	4.89	4.43	3.73	3.31
AlH_3-HCl	−32.98	−30.81	−30.42	−30.42	−29.99
AlH_3-H_2S	−15.91	−13.85	−13.36	−14.04	−14.17
AlH_3-PH_3	2.66	3.84	4.32	4.33	4.14

3.B. Dehydrogenation from BH_3-XH_m Complexes. The transition-state (TS) structures for model dehydrogenation reactions from BH_3-XH_m are portrayed in Figure 2, and the

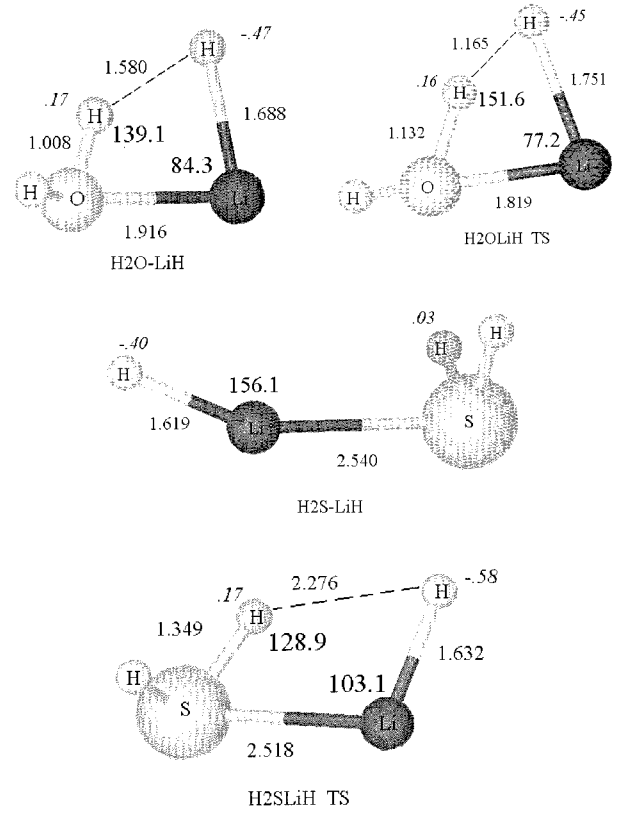

Figure 1. Equilibrium and transition-state structures of $LiH-H_2O$ and $LiH-H_2S$ at the MP2/6-311++G(2d,2p) level. The distances are in angstrom units, angles are in degrees (bold), and Mulliken atomic charges are shown in italics.

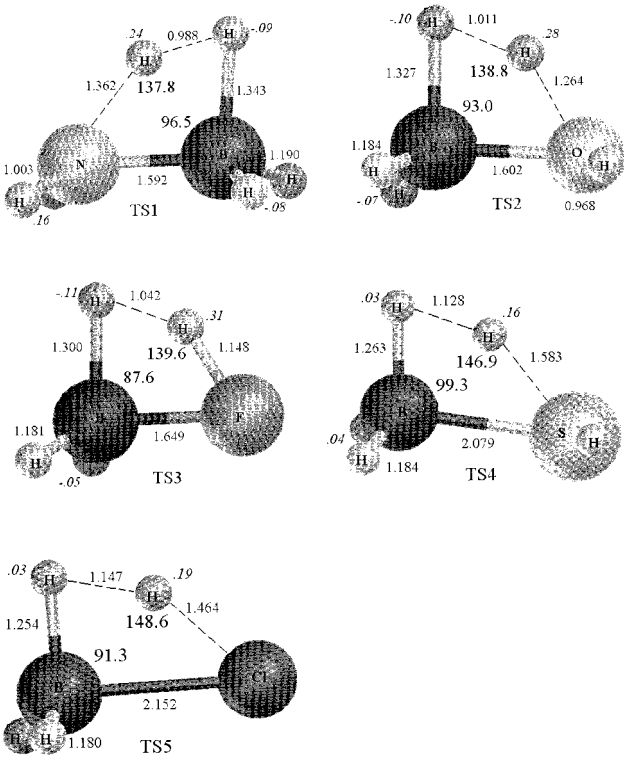

Figure 2. Transition-state structures for the dehydrogenation reaction $BH_3-XH_m \rightarrow BH_2-XH_{m-1} + H_2$ at the MP2/6-311++G(2d,2p) level. The distances are in angstrom units, angles are in degrees (bold), and Mulliken atomic charges are shown in italics.

corresponding barriers to dehydrogenation reactions are reported in Table 1. The H···H distances in the TS increase as the group of X is changed from BH_3-NH_3 to BH_3-HF. A similar trend is also seen for BH_3H_2S and BH_3-HCl, although the TS for dehydrogenation from BH_3-PH_3 could not be located at the MP2 level. For the TS of dehydrogenation of BH_3-HCl (cf. TS5 of Figure 2), the B−Cl bond has shortened substantially (0.554 Å) in the TS compared with that in the complex. A similar shortening of B−X bonds in BH_3-XH_m has been observed in all TS structures compared to their complexes. This shortening is considerable for the TS with X being halogens. For most of the structures of BH_3-XH_m, the X−H bonds involved in DH bonding are more elongated compared to their equilibrium distances (shown by dotted lines in Figure 2). Since the equilibrium structures of BH_3-XH_m complexes have staggered H−B···X−H bonds, they have higher barriers to dehydrogenation compared to $LiH-XH_m$ complexes. This is due to the requirement of undergoing rotation around B···X bond for a structure to be favorable for dehydrogenation (cf. Figure 2). The energies of the dehydrogenation reaction from BH_3-XH_m complexes in Table 2 indicate that reactions are exothermic.

3.C. Dehydrogenation from AlH_3-XH_m Complexes. Some important equilibrium and transition-state structures for model dehydrogenation reactions of AlH_3-XH_m are portrayed in Figure 3. For AlH_3-HF and AlH_3-HCl complexes the equilibrium structures have eclipsed geometry and H···H distances of 2.372 and 2.722 Å, respectively. The corresponding H···H distances in the TSs (TS8 and TS11 of Figure 3) are 1.199 and 1.297 Å, respectively. This large distance reorganization in the TSs along with the changes in the F/Cl−Al−H angle compared to the angles of corresponding complexes (cf. Figure 3) is expected to require more energy than in the case of the $LiH-H_2O$ complex. The expected trends are indeed observed in Table 1. However, for AlH_3-HF and AlH_3-HCl, the barriers to the dehydrogenation reaction are the least in the AlH_3-XH_m series (cf. Table 1). For other complexes, first they have to pass the barrier to rotation around the Al···X bond and further strengthen the intramolecular DHB to reach the transition state for the dehydrogenation reaction. Table 2 reveals that the dehydrogenation reactions from AlH_3-NH_3 and AlH_3-PH_3 are endothermic, whereas all other AlH_3-XH_m complexes have exothermic reactions.

Apart from the above-reported observations, some general salient features of the TSs for dehydrogenation are noteworthy. The shortest H···H bond distance in the TS for dehydrogenation is 0.988 Å (cf. TS1 for BH_3-NH_3 in Figure 2), whereas the longest is 1.297 Å (cf. TS11 for AlH_3-HCl in Figure 3). The DHB angle, (A)−H···H−X for the BH_3-XH_m series, is in the range 138−149°, whereas it is in the range 142−153° for the AlH_3-XH_m series. The barrier for dehydrogenation seems to be inversely proportional to the H···H bond distance in the TS. Energy barriers for the dehydrogenation reactions increase with a decrease in the electronegativity of the heteroatom, X of AH_n-XH_m, in a group as well as in the period. Further, for a given XH_m group in AH_n-XH_m, the dehydrogenation barrier decreases as the electropositive nature of A increases (cf. Table 1). The Mulliken charges for the TS structures indicate that in general the hydrogens involved in DHB have either more negative or positive charge compared to those hydrogen atoms not involved in DHB (cf. Figures 1−3). The natural charges for all equilibrium and TS structures have also been computed.[11] The trends in natural charges are analogous to those observed for Mulliken charges, implying suitability of Mulliken charges for the analysis in this case. The exothermicity of the dehydrogenation reaction seems to be decreasing in accordance with the electronegativity of X in the AH_n-XH_m complexes (cf. Table 2).

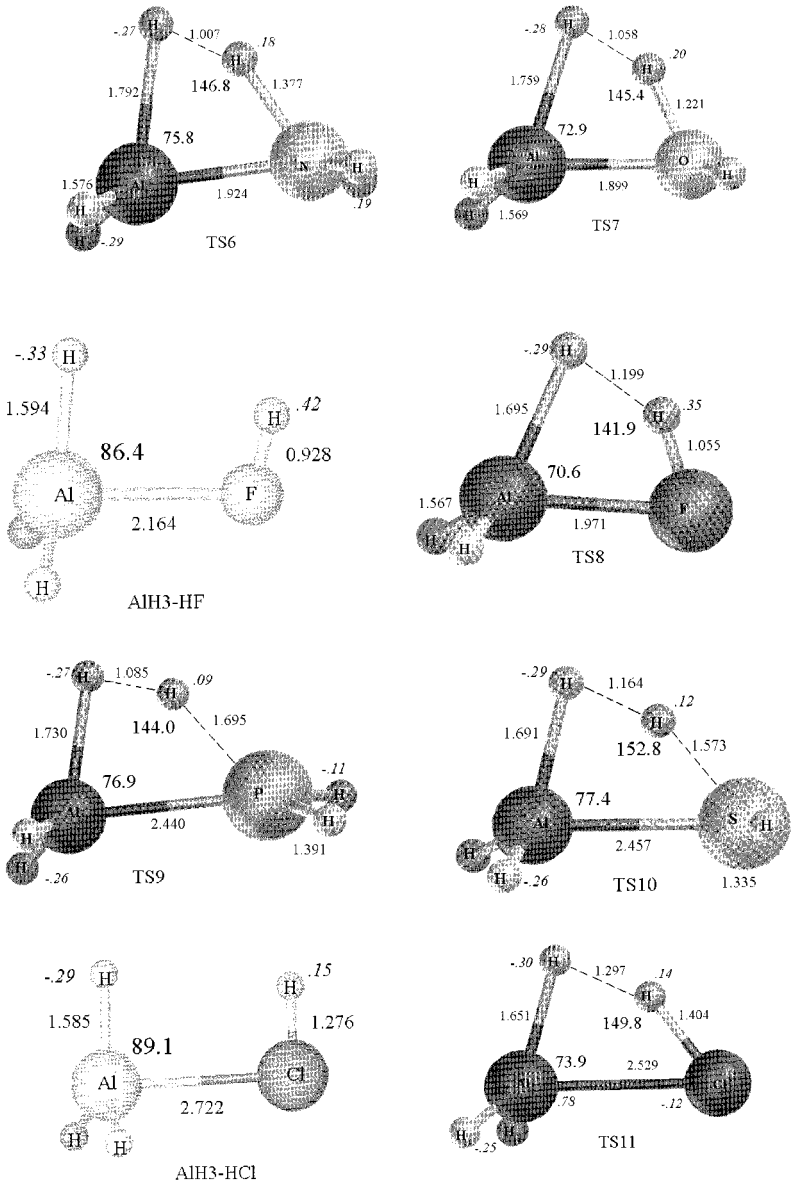

Figure 3. Some equilibrium and transition-state structures for the dehydrogenation reaction $AlH_3-XH_m \rightarrow AlH_2-XH_{m-1} + H_2$ at the MP2/6-311++G(2d,2p) level. The distances are in angstrom units, angles are in degrees (bold), and Mulliken atomic charges are shown in italics.

An attempt was made to analyze the model structure of piperidine−alane complex at the Hartree−Fock/6-31++g(d,p) level. However, the ab initio structure exhibits only the staggered configuration. This indicates that the stability of the experimentally observed eclipsed structure[6] may be due to its crystal environment.

4. Electron Density Analysis

The knowledge of bonding features of various structures involved in the dehydrogenation reaction including transition states is vital. This is made possible via a topographical analysis of the electron density distribution. The topographical analysis involves isolation and characterization of critical points (CPs) of ED. Critical points are those at which $\nabla\rho(\mathbf{r}) = 0$ and are characterized from the eigenvalues of the corresponding Hessian matrix[9] (a matrix of second-order partial derivatives). The existence of (3, −1) type CP between the two nuclei is an indicator of the existence of a bond between them and is termed a bond critical point (BCP). This property of ED is rather crucial because the mere existence of two nuclei in proximity does not necessarily mean the existence of a bond between them. Such bonding features have also been observed in our earlier studies,[4] especially in the case of seemingly bifurcated DHB. It is known from our earlier work[4] that the bonding patterns of intermolecular DHB are similar to that of the conventional hydrogen bond. In view of this, it is rather interesting to understand the bonding features of intramolecular dihydrogen bonding that exists in equilibrium structures as well as in the TS. The ED, its Laplacian, and bond ellipticity (defined from eigenvalues λ_i's of the Hessian matrix as $\epsilon = \lambda_1/\lambda_2 - 1$ with $|\lambda_1| > |\lambda_2|$) parameters have been used in the present analysis (cf. Table 3). The negative Laplacian is an indicator of a covalent bond, whereas a positive Laplacian indicates noncovalent interaction.[12] The bond ellipticity is a measure of stability, and the higher value indicates instability in the bond.[13]

The ED topographical analysis of equilibrium and TS structures that might have intramolecular DHB is presented in Table 3. In the case of $LiH-H_2O$, the TS has stronger Li−O and H···H bonds and weaker O−H(D) and Li−H(D) bonds than the corresponding equilibrium structure (cf. Table 3). The above observations in conjunction with the negative Laplacian of H··· H bond in TS indicate that the reaction has progressed in the

TABLE 3: Electron Density and Laplacian of Electron Density and Bond Ellipticities at the Bond Critical Points (BCP) of Some Complexes and Transition Structures of Dehydrogenation Reactions at the MP2/6-311++G(2d,2p) Level Geometry[a]

TS structure	location of CP[b]	$\rho(r)$	$\nabla^2\rho(r)$	ϵ	TS structure	location of CP[b]	$\rho(r)$	$\nabla^2\rho(r)$	ϵ
LiH−H_2O	Li−O bond	0.0285	0.2318	0.22	TS6	Al−N bond	0.0716	0.4011	0.16
	Li−H (D) bond	0.0340	0.1379	0.08		N−H (D) bond	0.1331	−0.1254	0.13
	O−H (D) bond	0.3168	−2.433	0.02		N−H bond	0.3471	−1.7803	0.03
	O−H bond	0.3752	−2.908	0.02		Al−H (D) bond	0.0484	0.1897	0.52
	H···H bond	0.0388	0.0453	0.12		Al−H bond	0.0834	0.2564	0.02
LiH−H_2O (TS)	Li−O bond	0.0376	0.3215	0.19		H···H bond	0.1426	−0.3391	0.07
	Li−H (D) bond	0.0301	0.1433	0.48	TS7	Al−O bond	0.0625	0.4336	0.13
	O−H (D) bond	0.2182	−1.057	0.02		O−H (D) bond	0.1709	−0.4022	0.07
	O−H bond	0.3749	−2.870	0.01		O−H bond	0.3700	−2.8560	0.01
	H···H bond	0.0901	−0.0806	0.05		Al−H (D) bond	0.5324	0.1923	0.29
LiH−H_2S	Li−S bond	0.0155	0.0739	0.02		Al−H bond	0.8394	0.2566	0.02
	Li−H bond	0.0386	0.1515	0.00		Al−H bond	0.8524	0.2608	0.02
	S−H bond	0.2200	−0.6534	0.13		H···H bond	0.1241	−0.2285	0.09
	S−H bond	0.2200	−0.6534	0.13	AlH_3−HF	Al−F bond	0.0224	0.1411	0.48
LiH−H_2S (TS)	Li−S bond	0.0149	0.0785	0.36		F−H (D) bond	0.3607	−3.581	0.00
	Li−H (D) bond	0.0382	0.1483	0.00		Al−H (D) bond	0.0799	0.2449	0.01
	S−H (D) bond	0.2162	−0.6230	0.12		Al−H bond	0.0833	0.2557	0.02
	S−H bond	0.2185	−0.6412	0.13	TS8	Al−F bond	0.0412	0.2963	0.47
	H···H bond	0.0139	0.0249	0.36		F−H (D) bond	0.2320	−1.4740	0.02
TS1	B−N bond	0.1365	0.3383	0.04		Al−H (D) bond	0.0632	0.2042	0.08
	N−H (D) bond	0.1384	−0.0616	0.53		Al−H bond	0.0859	0.2627	0.02
	N−H bond	0.3539	−1.8760	0.05		H···H bond	0.0866	−0.0448	0.16
	B−H (D) bond	0.1101	0.2607	0.21	AlH_3−HCl	Al−Cl bond	0.0152	0.0334	4.23
	B−H bond	0.1812	−0.2062	0.05		Cl−H (D) bond	0.2521	−0.7798	0.01
	H···H bond	0.1628	−0.3935	0.31		Al−H (D) bond	0.0815	0.2515	0.02
TS2	B−O bond	0.1088	0.4932	0.04		Al−H bond	0.0830	0.2551	0.02
	O−H (D) bond	0.1575	−0.1517	0.27	TS9	Al−P bond	0.0438	0.1123	0.20
	O−H bond	0.3744	−2.8921	0.01		P−H (D) bond	0.1066	−0.1381	0.19
	B−H (D) bond	0.1172	0.2041	0.04		P−H bond	0.1694	−0.1081	0.18
	B−H bond	0.1880	−0.2656	0.07		Al−H (D) bond	0.0549	0.1874	0.14
	H···H bond	0.1530	−0.3306	0.35		Al−H bond	0.0839	0.2574	0.01
TS3	B−F bond					H···H bond	0.1169	−0.1890	0.08
	F−H (D) bond	0.1822	−0.5097	0.11	TS10	Al−S bond	0.0383	0.1310	0.94
	B−H (D) bond	0.1285	0.1224	0.27		S−H (D) bond	0.1341	−0.2057	0.14
	B−H bond	0.1926	−0.3101	0.13		S−H bond	0.2159	−0.6158	0.05
	H···H bond	0.1372	−0.2395	0.37		Al−H (D) bond	0.0616	0.2105	0.16
TS4	B−S bond					Al−H bond	0.0844	0.2603	0.02
	S−H (D) bond	0.1324	−0.1503	0.42		H···H bond	0.0997	−0.1004	0.14
	S−H bond	0.2203	−0.6432	0.10	TS11	Al−Cl bond			
	B−H (D) bond	0.1391	0.1065	0.08		Cl−H (D) bond	0.1812	−0.4325	0.02
	B−H bond	0.1855	−0.2242	0.06		Al−H (D) bond	0.0692	0.2214	0.07
	H···H bond					Al−H bond	0.0856	0.2622	0.02
TS5	B−Cl bond					H···H bond	0.0713	0.0000	0.17
	Cl−H (D) bond	0.1599	−0.2873	0.12					
	B−H (D) bond	0.1456	0.0412	0.26					
	B−H bond	0.1887	−0.2421	0.14					
	H···H bond	0.1135	−0.0873	0.54					

[a] All values in atomic units. [b] (D) implies hydrogen expected to be involved in dihydrogen bonding.

direction of products. On the other hand, for LiH−H_2S, the equilibrium structure does not contain the DHB and in its TS the H···H bond is significantly longer having a small ED value and a positive Laplacian (closed-shell interaction) at the corresponding BCP analogous to intermolecular DHB observed in our earlier studies.[4] Similarly in the case of AlH_3−HF and AlH_3−HCl, the equilibrium structures do not contain the DHB, whereas their TSs show existence of DHB.

Some salient general features of the ED topography of intramolecular dihydrogen-bonded equilibrium and TS are noteworthy. The short H···H distances in the TS are reflected by their negative Laplacian values, with the exception of the TS of LiH−H_2S and AlH_3−HCl. This indicates that the covalent character has encrypted in the H···H bond of most of the TS and that the reaction has proceeded toward the product after passing through the phase of DHB (although stationary structures proving this point are rather rare, e.g., LiH−H_2O complex in this case). As the H···H bond becomes shorter, it has more ED value at the BCP. For TS structures of LiH, BH_3, and AlH_3 complexes, more ED gets localized in the H···H bond as one goes from their complexes with HF to NH_3 as well as HCl to PH_3 and is reflected in their ED values and Laplacian (bond has acquired more covalent character). Further, the bond ellipticity values are greater for a weaker bond (having less ED at the H···H BCP). The ED topography of TS of BH_3−HF, BH_3−HCl, BH_3−H_2S, and AlH_3−HCl shows the absence of BCP corresponding to the A···X bond. This could be a result of a shifting of the A···X bond ED in the H···H bond region for the stability of the structure. In the case of BH_3−H_2S (TS4), the DHB could not be observed despite an H···H distance of 1.128 Å.

5. Concluding Remarks

The possibility of the existence of intramolecular dihydrogen bonding is explored for main group elements at the ab initio level of theory. The equilibrium structures of LiH−H_2O, AlH_3−HF, and AlH_3−HCl complexes have eclipsed the H−A···X−H structure and therefore have feasibility for intramolecular DHB. These complexes undergo dehydrogenation reactions fairly

easily with smaller activation barriers compared to those with staggered equilibrium configurations. The relatively high barrier for dehydrogenation for staggered equilibrium structures may be attributed to their requirement of surpassing the barrier for rotation around the A···X bond before reaching the H···H bonded TS. The ED analysis of TS structures reveals that they are late TS, since the H···H bond shows more covalent character and further supports the existence of DHB in the TS for dehydrogenation. Thus, to facilitate the dehydrogenation from complexes of type AH_n-XH_m, the formation of intramolecular DHB is vital and seems to be a driving force for the reaction. Under the environment provided by the crystal field, the forces may become favorable to stabilize the eclipsed structures, leading to the intramolecular DHB observed in several studies.[6−7]

Acknowledgment. The author is grateful to Professor S. R. Gadre (Pune University) for the computational facility as well as support and to Mr. Avinash Marathe (MBT, Pune) for constant encouragement. The author is thankful to one of the referees for his suggestions, which resulted in the addition of a topographical analysis of electron density in the revised version.

References and Notes

(1) Jeffrey, G. A. *An Introduction to Hydrogen Bonding*; Oxford University Press: Oxford, 1997.

(2) Crabtree, R. H.; Siegbahn, P. E. M.; Eisenstein, O.; Rheingold, A. L.; Koetzle, T. F. *Acc. Chem. Res.* **1996**, *29*, 348. Crabtree, R. H. *Science* **1998**, *282*, 2000.

(3) Richardson, T. B.; deGala, S.; Crabtree, R. H.; Siegbahn, P. E. M. *J. Am. Chem. Soc.* **1995**, *117*, 12875. Alkorta, I.; Elguero, J.; Foces-Foces, C. *Chem. Commun*. **1996**, 1633. Alkorta, I.; Rozas, I.; Elguero, J. *Chem. Soc. Rev*. **1998**, *27*, 163.

(4) Kulkarni, S. A. *J. Phys. Chem. A* **1998**, *102*, 7704. Kulkarni, S. A.; Srivastava, A. K. *J. Phys. Chem. A* **1999**, *103*, 2836.

(5) Stevens, R. C.; Bau, R.; Milstein, D.; Blum, O.; Koetzle, T. F. *J. Chem. Soc., Dalton Trans*. **1990**, 1429. Van der Sluys, L. S.; Eckart, J.; Eisenstein, O.; Hall, J. H.; Huffman, J. C.; Jackson, S. A.; Koetzle, T. F.; Kubas, G. J.; Vergamini, P. J.; Caulton, K. G. *J. Am. Chem. Soc*. **1990**, *112*, 4831. Peris, E.; Lee, J. C., Jr.; Rambo, J.; Eisenstein, O.; Crabtree, R. H. *J. Am. Chem. Soc*. **1995**, *117*, 3485.

(6) Atwood, J. L.; Koutsantonis, G. A.; Lee, F.; Raston, C. L. *J. Chem. Soc., Chem*. *Commun*. **1994**, 91.

(7) Padilla-Martinez, I. I.; Rosalez-Hoz, M. J.; Tlahuext, H.; Camacho-Camacho, C.; Ariza-Castolo, A.; Contreas, R. *Chem. Ber*. **1996**, *129*, 441.

(8) Frisch, M. J.; Trucks, G. W.; Schlegel, H. B.; Gill, P. M. W.; Johnson, B. G.; Robb, M. A.; Cheeseman, J. R.; Keith, T.; Petersson, G. A.; Montgomery, J. A.; Raghavachari, K.; Al-Laham, M. A.; Zakrzewski, V. G.; Ortiz, J. V.; Foresman, J. B.; Peng, C. Y.; Ayala, P. Y.; Chen, W.; Wong, M. W.; Andres, J. L.; Replogle, E. S.; Gomperts, R.; Martin, R. L.; Fox, D. J.; Binkley, J. S.; Defrees, D. J.; Baker, J.; Stewart, J. J. P.; Head-Gordon, M.; Gonzalez, C.; Pople, J. A. *Gaussian 94*, revision B.3; Gaussian, Inc.: Pittsburgh, PA, 1995.

(9) Bader, R. F. W. *Atoms in Molecules: A Quantum Theory*; Clarendon: Oxford, 1990. The critical points of molecular electron density distribution (ED) can be characterized from its rank and signature (excess of positive eigenvalues over negative ones). Thus, maxima are denoted as (3, −3), minima are denoted as (3, +3), and two types of saddles are denoted as (3, −1) and (3, +1). The ED is maximum at the nuclear sites, and a (3, −1) saddle is found between every bonded pair of atoms (called bond critical point). The presence of a ring or cage in the system can be identified from the occurrence of a (3, +1) saddle and minimum in the ED distribution.

(10) Program UNIPROP developed by Gadre and co-workers at University of Pune, Pune, India for calculating topographical properties of electron density, electrostatic potential, and electron momentum densities. Nonnegative scalar fields such as electron density satisfies the Poincare−Hopf relationship (see ref 9) $n_{-3} - n_{-1} + n_{+1} - n_{+3} = 1$, where n_{-3} is the number of maxima, n_{-1} is the number of (3, −1) CPs, n_{+1} is the number of (3, +1) CPs, and n_{+3} is the number of minima.

(11) Weinhold, F.; Carpenter, J. E. *The Structure of Small Molecules and Ions*; Plenum: New York, 1988.

(12) Bone, R. G. A.; Bader, R. F. W. *J. Phys. Chem*. **1996**, *100*, 10892. Bader, R. F. W.; Essen, H. *J. Chem. Phys*. **1984**, *80*, 1943.

(13) Koch, U.; Popelier, P. L. A. *J. Phys. Chem.* **1995**, *99*, 9747. Popelier, P. L. A. *J. Phys. Chem*. **1998**, *102*, 1873.